SCIPP 94/34
October 1994

Signal-to-Noise in Silicon Microstrip Detectors with Binary Readout

J. DeWitt, D. Dorfan, T. Dubbs, A. Grillo, B. Hubbard, S. Kashigin, K. Noble, T. Pulliam, J. Rahn, W. A. Rowe, H. F.-W. Sadrozinski, A. Seiden, E. Spencer, A. Webster, M. Wilder, D. C. Williams
SCIPP, University of California, Santa Cruz, CA USA
A. Ciocio, T. Collins, I. Kipnis, H. Spieler, *Lawrence Berkeley Laboratory, Berkeley, CA, USA*
H. Iwasaki, T. Kohriki, T. Kondo, S. Terada, Y. Unno, *KEK, Tsukuba,Japan*
Y. Iwata, T. Ohmoto, T. Ohsugi, M. Yoshikawa, *Hiroshima University, Hiroshima, Japan*
R. Takashima, *Kyoto University of Education, Kyoto, Japan*
H. Maeohmichi, M. Takahata, N. Tamura, *Okayama University, Okayama, Japan*

Abstract·

We report the results of a beam test using double-sided AC-coupled silicon microstrip detectors with binary readout, i.e., a readout where the signals are discriminated in the front-end electronics and only the hit location as kept.

For strip pitch between 50μm and 200μm, we determine the efficiency and the noise background as function of threshold setting. This allows us to reconstruct the Landau pulse height spectrum and determine the signal/noise ratio. In addition, the threshold/noise ratio necessary for operation with low occupancy is determined.

I. INTRODUCTION

In proposed silicon tracking detectors at future large hadron colliders [1], the front end electronics (FEE) has to be efficient and has to control the noise background in the anticipated large number of channels. One possible choice is the so-called "binary read-out" where the pulse from the silicon detector is amplified and then compared with a threshold, preferably in the same ASIC chip to preserve the matching of the circuit components on one chip. The location and time stamp (but not the pulse height) of pulses exceeding the threshold are kept and stored in a digital pipeline for readout after a valid trigger. Obviously, in this procedure, information is lost which might be present in a fully analog system. This is first the pulse height (beyond the fact that the pulse height exceeded the threshold or not), and secondly the correlation of noise in different channels, for example, if generated by common modes. For operation of a large system, the loss of information necessitates careful matching of the thresholds and control of the noise, especially common mode noise. The advantage of the binary system is the simplicity of the FEE, minimal requirements for the pipeline and data transmission, lower power consumption, less material and lower cost.

The single channel noise of the FEE system can be determined accurately in the laboratory using the calibration system. In order to understand the response of silicon detectors to minimum ionizing particles [MIP's], we performed a beam test in the 4GeV π^- beam at KEK, a continuation of previous beam tests to evaluate detector and FEE prototypes for high luminosity application[2]. The use of MIP's normalizes the charge scale of the noise measurement to that of the pulse height measurement of the MIP signal; the signal-to-noise ratio can be determined and the efficiency and noise occupancy as a function of threshold evaluated.

Instrumenting about 1000 channels of low-noise FEE and detectors addresses the system aspects of binary readout schemes. This includes the question of matching gain and noise over several chips. Large scale silicon microstrip systems based on the binary readout scheme are now also operating under experimental conditions[3].

II. BEAM TEST SET-UP

The set-up of the beam test was very similar to our previous test at KEK[2]: the 4GeV π^- beam was defined by a pair of scintillation counters of about 5mm x 10mm area, which, in coincidence, supplied a trigger which initiated the readout. The phase of the trigger signal relative to the phase of the clock was measured in a TDC.

Four planes of silicon microstrip detectors were arranged between the trigger counters. Here we will discuss results only from three which have identical FEE systems, as indicated in Fig.1. The two outside planes acted as anchors and had identical bonding arrangements. The inner detector plane, the device under test, DUT, was located in between and had varying strip pitch as explained below.

The detectors[4] have been developed by Hamamatsu Photonics for use in high luminosity colliders. They are double-sided AC-coupled detectors with 50 μm pitch and narrow implants to minimize the interstrip capacitance and hence single channel noise. The n-side is axial, and the p-side has a 10mrad stereo angle. Their depletion voltage is about 70V, and we have varied the bias voltage in our test. Here, we report on measurements with a bias voltage of 100V.

The silicon detectors are 6cm long and 3.4cm wide, but we instrumented only the central part of both sides of each detector with 128 channels of fast low-power, low-noise FEE, consisting of a bipolar amplifier-comparator ASIC (LBIC)[5] and a CMOS 40MHz Digital Pipeline (CDP64)[6], both having 64 channels and designed to support 50μm detector pitch. Details of the FEE system an be found in Refs. [5] and [6], so here we give only the essential properties: the rise time

· Presented at the 1994 IEEE Nuclear Sciences Symposium, Norfolk, VA.

is 20ns, the double hit resolution is 60ns, and the input noise charge as function of external capacitance C is $\sigma_{noise}=640+32*C$ [electrons].

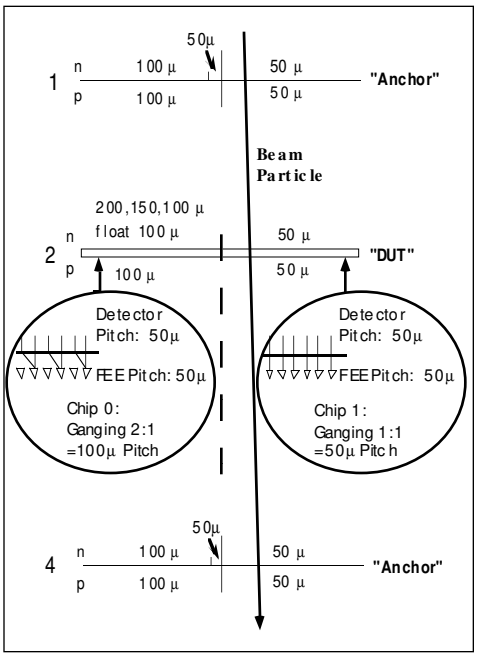

Fig.1 Set-up of the KEK beam test. The outer two detectors serve as "anchors", the inner is the device under test, DUT. Note the areas of different pitch.

Because we wished to measure efficiencies as a function of pitch, we employed different bonding schemes between detector strips and FEE channels, as shown in Fig.1. On one chip per side and plane, every strip was bonded to a corresponding FEE channel with 50µm pitch. The other chip had a varying number of strips ganged and then bonded to a common FEE channel, thus simulating larger detector pitch. The two anchor planes and the p-side of DUT had 100µm pitch connected to the second chip. The n-side of DUT had a strip pitch between 100, 150 and 200µm, which in the following will also be called "100µm pitch". The arrangement with floating strips on the DUT will not be discussed here.

III. CALIBRATION: GAIN and NOISE

The FEE is calibrated by applying a pulsed voltage signal to the calibration capacitor of close to 90fF at the input of every channel, which injects a known charge into the channel.

By measuring the occupancy as function of the threshold voltage for several calibration inputs (Q_{in}=0.6, 1.1, 1.5, 2.1, 3.1, 4.5 fC, Fig.2), the gain and input noise of the amplifier-comparator is determined: we fit the curves in Fig.2 to error functions, which are characterized by the threshold voltages at 50% occupancy, which we call the response, and the output noise sigma σ_n, which is related to the width of the curves - for instance, the difference between the 88% and 12% occupancy points is $2.37*\sigma_n$=FWHM.

Fig.3a shows the response, in mV, and Fig.3b shows the small signal gain, in mV/fC, which is the derivative of the response curve, and translates the variations in threshold over the range of the width of the error functions into variations of charge at the input. We then divide the output noise, in mV, (Fig.3c) by the small signal gain (Fig.3b) to get the noise at the input σ_o, in fC, (Fig.3d).

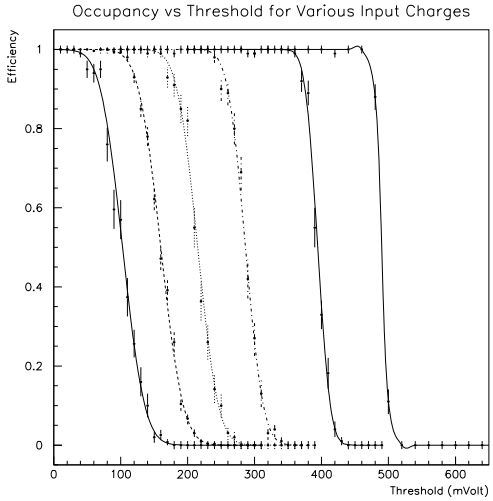

Fig.2 Occupancy vs threshold voltage for various calibration input charges: Q_{in}=0.6, 1.1, 1.5, 2.1, 3.1, 4.5 fC. The curves are fits to error functions.

As seen in Fig.3a, the response is non-linear (by design, in order to save power), and thus the small signal gain (Fig.3b) is not constant as a function of input charge. On the other hand, the output noise (Fig.3c) is not constant either, and so we find that the noise at the input σ_o (Fig.3d) is independent of the charge of the input signal, a necessary condition for the calibration method to be useful in measuring the noise.

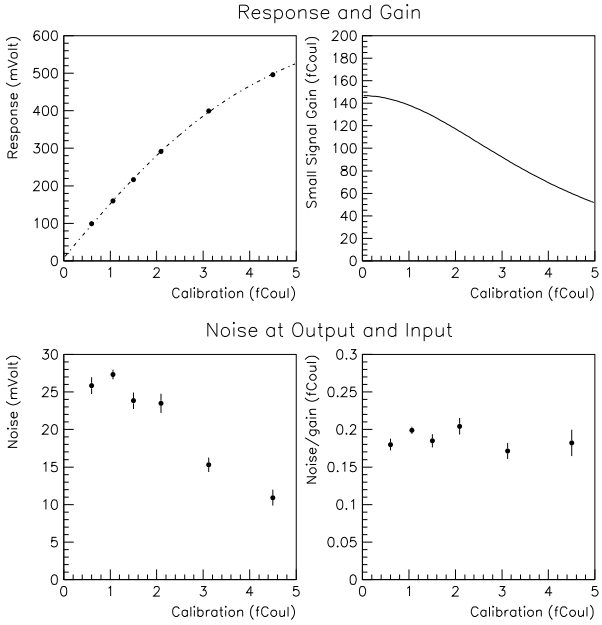

Fig. 3 Extraction of the response and input noise as function of input charge: a) response , b) slope of the response curve = small signal gain, c) noise at the output, d) input noise.

In Ref.[5], a correction to the gain as determined by the calibration method is calculated: the effective charge is about 84% of the input charge. This correction has been applied in the following.

The matching of the response across two chips on the p-side of the DUT is shown in Fig.4a, and the corresponding matching of the input noise is shown in Fig.4b, both for a 1fC input charge. In Ref.[5], it was shown that the matching is as good as 3.5% in the response, given that the calibration circuits are carefully measured.

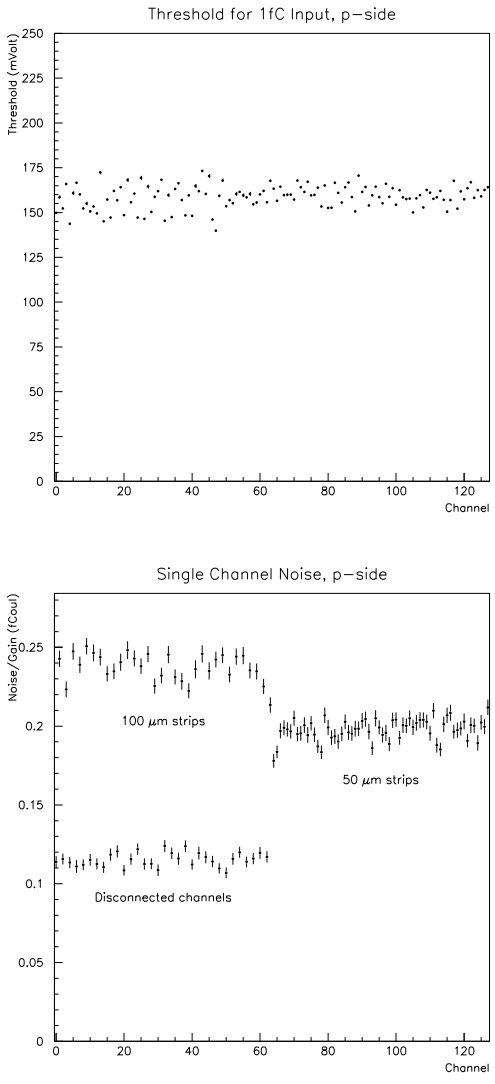

Fig. 4 Matching of response and input noise for the two 64 channel chips on the p-side of DUT at an input charge of 1fC: a) response b) input noise.

Note that we expect a detector with true 100μm pitch and optimized implant width to have smaller noise than our case of two ganged 50μm strips, in fact having noise close to our case of a single strip with 50μm pitch.

Using the response function and the small signal gain, we can refer the threshold to the input charge, thus in the following, we will express the threshold setting in terms of input charge, in fC, instead of voltage.

IV. EFFICIENCY AND OCCUPANCY AS FUNCTION OF THRESHOLD

Data Reduction

To study the performance of the detectors, the first step was to locate active time slices, identify bad channels, and align the planes to each other. In order to study time-walk effects and because of timing differences between the different amplifiers tested, ten 40 MHz time slices were read out for each trigger. For LBIC chips on the n-side of each detector, the data is confined within four time slices. For the p-side, it is confined within five. For the present analysis, we have OR'ed these time slices. Because the pulse width of the LBIC is of the order of 60ns, we expect about three time slices to be filled by the signal from one track. We will have to investigate the time walk of the amplifier and the time jitter due to the asynchronous arrival of beam particles relative to the clock of the digital pipeline.

Once the time slices are established, the data is searched for dead or noisy channels and the readout map cross-checked. Using 57,000 pion events at nominal threshold and bias, the number of hits in each channel connected to a detector strip is recorded. Any channel with less than one hit for every 300 events is considered dead and any channel with more than one hit per five events is considered hot. A complete survey of all three planes with LBIC amplifiers identified only one dead channel out of 768 and no hot channels. For reasons that are still under investigation, a few unconnected channels show small occupancies (~5%).

To study the performance of the detectors in detail, the middle detector (DUT) must be aligned with respect to the two outer. For perfectly aligned detectors, the pion's point of intersection in the DUT, x_2, can be predicted from measurements in the two outer detectors, x_1 and x_4

$$x_2 = (1/3)(x_1+2*x_4) \qquad (1)$$

Misalignments result in a difference between the measured and predicted position x_2 and take two forms: offset and rotation. To check for rotational misalignments it is necessary to use the 10 milliradian stereo angle between the n and p sides of each detector to measure the particle's trajectory in the dimension perpendicular to the strips. When the particle trajectories in this dimension is compared to the difference between predicted and measured position x_2, no apparent correlation is seen. This indicates that the detector plans have no visible rotation with respect to each other.

Since no rotational alignment is necessary, the offset alignment and the resolution of the detectors can be measured by directly comparing the expected and measured position. For the p-side, resolutions of 17.6 and 29.5 μm are seen for the 50 and 100 μm strips, respectively. Dividing by the square root of the sum of weights squared of eq.(1), i.e. sqrt(14/9), we find single strip resolutions of 14.1 and 23.7μm in reasonable agreement with the expected resolution of strip pitch divided by sqrt(12).

Efficiency and Background at Nominal Threshold and Bias

Hit positions and resolutions in each detector plane are measured by clustering together adjacent channels with signals above threshold. For the purposes of measuring efficiencies and background, any event where a cluster is found adjacent to a bad channel or to an unconnected strip is rejected. A further requirement is that one and only one hit is found on each of the outer planes.

To measure the efficiency, the hits in the outer planes along with the alignment results are used to predict which strip the particle will strike in DUT. A search is made within a +/- 3 strip margin for a matching hit. If none is found the event is considered inefficient, as long as there are no dead or disconnected strips inside this margin. If a hit is found a second search is made for any hits outside +/- 4 strips. Each hit found outside this margin is considered background.

Out of 57,000 events at a threshold of 1.0 fC, 7,000 events where rejected and only 19 events where inefficient on the p-side of plane 2. This corresponds to an efficiency of 99.96%. Of the accepted events, 284 background hits were found in the 50µm strips and 332 on the 100µm strips. Dividing by the number of channels and by an addition factor of two to approximately account for the integration over several time slices, this corresponds to a background rate per strip of $0.5*10^{-4}$ and $1.2*10^{-4}$ for the 50 and 100µm strips respectively.

Performance on the n-side is comparable: 20,000 events were rejected (13,000 to avoid the floating strips on part of the detector) and 110 events were inefficient. This corresponds to an efficiency of 99.73%. Background rates were measured at $0.5*10^{-4}$ and $2.4*10^{-4}$ for the 50µm and 100/150/200µm strips respectively.

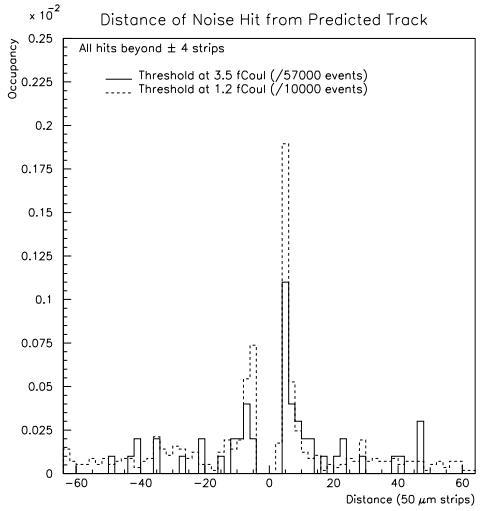

Fig.5 Distance of noise hit from predicted track, for 1.2fC and 3.5fC threshold. Note the increased occupancy close to the track.

Although the background rates were low, they are still higher than expected from white noise. When the position of the noise hit is plotted with respected to the predicted location of the particle (Fig.5), large peaks near zero suggest a physical source for the background, perhaps δ-rays or nuclear showers. In the following, we determine the occupancy due to noise by searching for extra hits outside of +-10 strips.

Results at Various Thresholds

The signal-to-noise ratio can be investigated by varying the threshold. The result is the efficiency and background curves shown in Figs.6 and 7. Fig.6a shows the efficiency and Fig.6b the occupancy for the p-side of DUT, while Figs.7a and 7b show the efficiency and occupancy for the n-side. In all cases, curves for 50µm and 100µm are shown, (recall that for the n-side, "100µ strips" stands for 100/150/200µm).

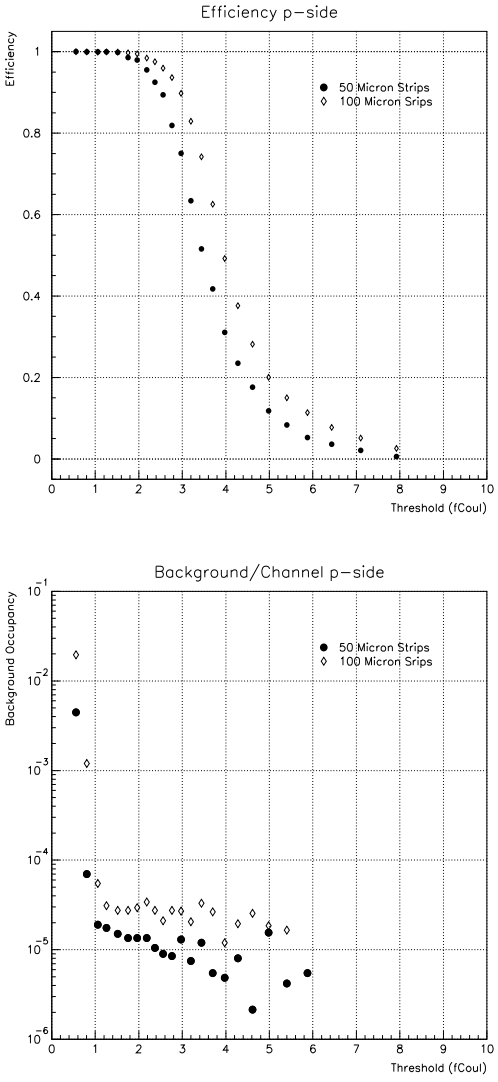

Fig. 6 a) Efficiency and b) occupancy in two 40MHz time buckets outside +- 10 strips for the p-side as function of threshold .

In all cases, there is a comfortable operating range with low noise and high efficiency. The results for efficiency ε and occupancy O are summarized in Table 1 for two threshold values.

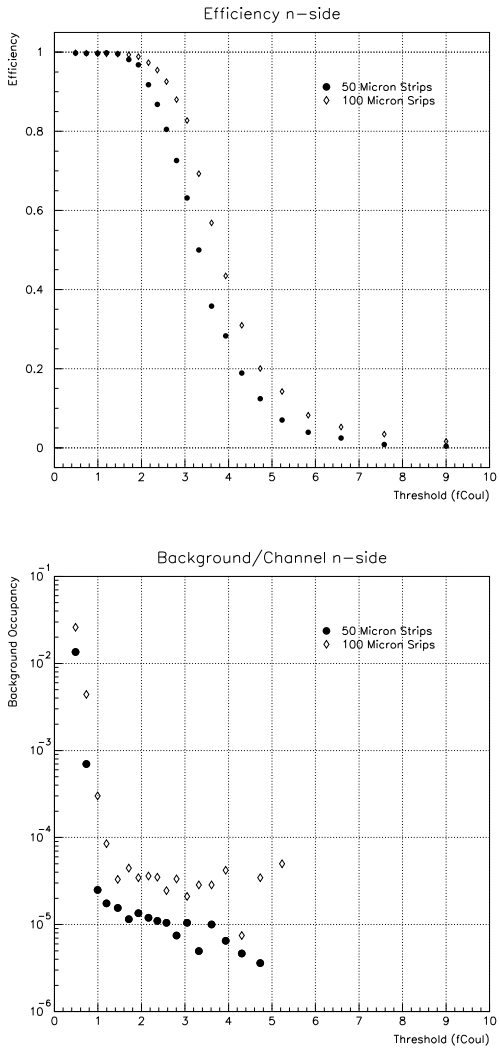

Fig. 7 a) Efficiency and b) occupancy in two 40MHz time buckets outside +- 10 strips for the n-side as a function of threshold .

Table 1 : Efficiency ε and Occupancy O for different Pitch and two Thresholds

Pitch [μm]	V_{th} [fC]	$\varepsilon(p)$ [%]	$O(p)$ [10^{-4}]	$\varepsilon(n)$ [%]	$O(n)$ [10^{-4}]
50	1	99.98	0.2	99.7	0.25
50	2	98.0	0.13	96.8	0.13
100	1	99.92	0.7	−−	−−
100	2	99.5	0.3	−−	−−
100 / 150 / 200	1	−−	−−	99.6	3.0
100 / 150 / 200	2	−−	−−	98.8	0.4

For a threshold of 1fC, the efficiency is in excess of 99%, both for n- and p-side, for both values of the pitch. The occupancy level is below 10^{-3} for all cases, and typically less than 10^{-4}. Even for a threshold of 2fC, the efficiencies are above 95%, and above 99% for 100µm pitch, coupled with occupancies of a few times 10^{-5}.

Pulse Height Distribution

The efficiency as a function of threshold (Fig. 6a and 7a) is the integral spectrum of the pulse height. A simple way of recovering the pulse height spectrum is to approximate a differentiation by subtracting the efficiency at each threshold value from that at the preceding one. The results, shown in Figs.8a,b for the p- and n-side, respectively, resembles the expected Landau distribution.

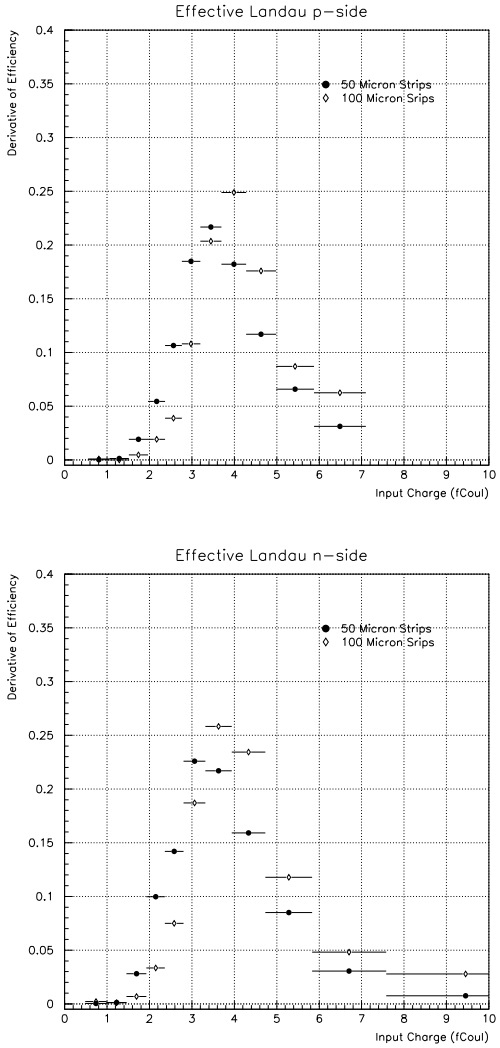

Fig. 8 Pulse Height spectrum of MIP's for two different pitches: a) p-side, b) n-side of DUT.

A few features should be noted: due to charge sharing between two strips, the distribution is not an exact Landau and we observe differences between the 50 and 100µm pitch case. The median of the distributions are close to 4fC as expected for a Landau distribution (see Table 2). Thus we find that the pulse height scale derived from the beam and the input charge scale derived from the calibration agree.

Signal / Noise and Threshold / Noise Ratio's

Using the efficiency and occupancy curves as a function of threshold, two important numbers for the design and operation of a large system can be determined. One is the value of the signal-to-noise ratio, the other the threshold-to-noise ratio necessary for low occupancy. Defining as the signal S the median of the pulse height distribution (Fig.8), i.e., the 50% point of the efficiency curves Figs.6a and 7a, and taking the noise N = σ_{noise} from the calibration runs, we can evaluate the signal-to-noise ratio S/N separately for n- and p-side and different pitches. This is shown in Table 2. As pointed out before, the noise of our 100μ pitch configuration made of two ganged 50m pitch strips is larger than for a true 100μ pitch detector.

Note that this ratio includes all effects, for example, noise due to the capacitance, strip resistance, and neighboring channels as well as signal loss due to sharing between the neighbors, due to AC-coupling and the ballistic deficit.

Table 2: Signal-to-Noise Ratios S/N

p / n	*Pitch* [μm]	σ_{noise} [fC]	*S* [fC]	*S / N*
p	50	0.16	3.5	22
p	100	0.21	4.0	19
n	50	0.21	3.4	16
n	100 / 150 / 200	0.21 – 0.26	3.7	15

The S/N ratio is degraded on the n-side mainly because of the poorer noise performance due to the larger interstrip capacitance. Because of the increased capacitance of ganged strips, the signal-to-noise ratio is lower for wider pitch. The occupancy curves as a function of threshold Figs.6b and 7b allow the determination of the threshold value at which the noise occupancy O falls below an acceptable level. This level is about O < 10^{-3} for LHC application, because it is below the occupancy due to the p-p interactions. The noise rate and thus the occupancy O is an approximate Gaussian as function of the threshold-to-noise ratio:

$$O = O_o \cdot e^{\frac{-V^2_{th}}{2\sigma^2_{noise}}} \quad . \qquad (2)$$

Thus, one expects that the same noise level is reached for the same threshold-to-noise ratio, independent of the absolute value of the noise sigma.

Table 3: Threshold-to-Noise Ratio for Occupancy O = 10^{-3} in two 40MHz Bins

p / n	*Pitch* [μm]	σ_{noise} [fC]	V_{th} [fC]	V_{th} / σ_{noise}
p	50	0.16	0.65	4.0
p	100	0.21	0.80	3.8
n	50	0.21	0.75	3.6
n	100 / 150 / 200	0.21 – 0.26	0.90	3.8

In Table 3, we show the threshold-to-noise ratio V_{th}/σ_{noise} for p- and n-side and two different values of pitch for O = 10^{-3} and conclude that values close to 4 are required.

V. CONCLUSIONS

In a beam test, we have verified the proper functioning of 6cm long double-sided, AC-coupled Silicon Microstrip detectors with binary readout, consisting of a bipolar amplifier-comparator and a CMOS digital pipeline, operating at 40MHz.

We have determined the efficiency and occupancy as a function of the single threshold in the system, for both n-side and p-side and a pitch of 50,100 and up to 200μm. At 30V over depletion, the efficiency with a 1fC threshold is above 99% with a occupancy in two 40MHz time slices of less than 10^{-3}, for both the p- and n-side and 50 and 100μm pitch. For a threshold of 2fC, the efficiency is larger than 95%. The occupancy is O < 0.1% with a threshold-to-noise ratio greater than about 4.0.

The Landau distribution peaks close to the expected value of 4fC and we find signal-to-noise ratio's S/N=19-22 for the p-side and S/N=15-16 for the n-side, depending on the pitch. Smaller pitch has better S/N because the pulse height loss due to charge sharing is off-set by a reduced capacitance. This conclusion is expected to change when strips with 100μm pitch and optimized geometry are used, where the capacitance will be much smaller than in our case with two ganged strips.

The position resolution was measured on the p-side and is slightly better than pitch divided by sqrt(12).

In the future, we will investigate the dependence of the efficiency on bias voltage, angle of incidence, strip geometry, detector properties, radiation history for both junction and ohmic side.

VI. ACKNOWLEDGMENTS

This work was supported in part by the US. Department of Energy, the US-Japan Collaborative Program and the Joint Research of the International Scientific Research Program, Ministry of Education, Science and Culture, Japan.

VII. REFERENCES

[1] ATLAS Collaboration, Status Report, CERN/LHC/92-24.
[2] Y. Unno *et al*, Beam Test of the SDC Double-sided Silicon Strip Detector, KEK Preprint 93-127, Oct. 1993.
[3] E. Barberis *et al*., Design, Testing and Performance of the FEE for the LPS Silicon Microstrip Detectors, SCIPP 94/29.
[4] T. Ohsugi *et al.*, Double-sided Microstrip Sensors for the Barrel of the SDC Silicon Tracker, Nucl. Instrum. Methods **A342** (1994) 16.
[5] E. Spencer *et al.*, A Fast Shaping Low-Power Amplifier-Comparator Integrated Circuit for Silicon Strip Detectors, IEEE N.S. Symp., Norfolk, VA , 1994, SCIPP 94/32.
[6] J. DeWitt, A Pipeline and Bus Interface Chip for Silicon Strip Detector Readout, IEEE N.S. Symp., San Francisco, CA, Nov. 1993, SCIPP 93/37.